frontiers | Frontiers in Physics

TYPE Original Research
PUBLISHED 25 October 2022
DOI 10.3389/fphy.2022.1054299

OPEN ACCESS

EDITED BY
Bernard Gelloz,
Nagoya University, Japan

REVIEWED BY
Lingzhen Guo,
Max Planck Institute for the Science of Light, Germany
F. Nori,
RIKEN, Japan

*CORRESPONDENCE
Y. Q. Zhang,
lanzhougx@163.com

SPECIALTY SECTION
This article was submitted to Optics and Photonics,
a section of the journal
Frontiers in Physics

RECEIVED 26 September 2022
ACCEPTED 11 October 2022
PUBLISHED 25 October 2022

CITATION
Zhang YQ, Zhu ZH, Chen KK, Peng ZH, Yin WJ, Yang Y, Zhao YQ, Lu ZY, Chai YF, Xiong ZZ and Tan L (2022), Controllable single-photon routing between two waveguides by two giant two-level atoms.
Front. Phys. 10:1054299.
doi: 10.3389/fphy.2022.1054299

Controllable single-photon routing between two waveguides by two giant two-level atoms

Y. Q. Zhang[1,2]*, Z. H. Zhu[1,2], K. K. Chen[1,2], Z. H. Peng[1,2], W. J. Yin[1,2], Y. Yang[1,2], Y. Q. Zhao[1,2], Z. Y. Lu[1,2], Y. F. Chai[1,2], Z. Z. Xiong[3] and L. Tan[4]

[1]School of Physics and Electronics Science, Hunan University of Science and Technology, Xiangtan, China, [2]Hunan Provincial Key Laboratory of Intelligent Sensors and Advanced Sensor Materials, Xiangtan, China, [3]School of Physics and Electronics, Gannan Normal University, Ganzhou, China, [4]Institute of Theoretical Physics, Lanzhou University, Lanzhou, China

We investigate the single-photon quantum routing composed of two infinite waveguides coupled to two giant two-level atoms. The exact expressions of the single-photon transmission and reflection amplitudes are derived with the real-space approach. It is found that the single photon scattering behavior is strongly dependent on the phase difference between the two adjacent atom-waveguide coupling points, the frequency detuning, the coupling strength between the two giant atoms, and the interaction strengths between the giant atoms and the waveguides. Our studies show that an ideal single photon router with unit efficiency can be realised by designing the size of the giant atom, and the frequency detuning or adjusting the interaction strengths between the atoms and the waveguides. The results suggest the potential to effectively control the single-photon quantum routing based on the giant-atom setup.

KEYWORDS

giant two-level atom, single photon, qantum routing, phase difference, waveguide

1 Introduction

The design and realization of scalable quantum information processing systems rely on quantum networks [1]. As an essential ingredient in a quantum network, quantum routers can be used to transfer the quantum information from one channel to others, distributing it in the network. Due to their fastness, very low loss and long-playing coherence [2–4], photons are considered as ideal candidates of carriers of quantum information and thus quantum routing of photons has drawn more attentions in recent years. Numerous theoretical and experimental researches on quantum routing or photon transport have been made based on several different structures, such as coupled-resonator waveguides [5–16], whispering-gallery-mode resonators [17–20], waveguide-emitter systems [21–29], superconducting circuit [30–36].

Recently, giant atoms, as an emerging playground in quantum optics, have attracted a plethora of research interest because they exhibit several striking new phenomena, such as frequency-dependent relaxation rate and Lamb shift [37,38], oscillating bound states

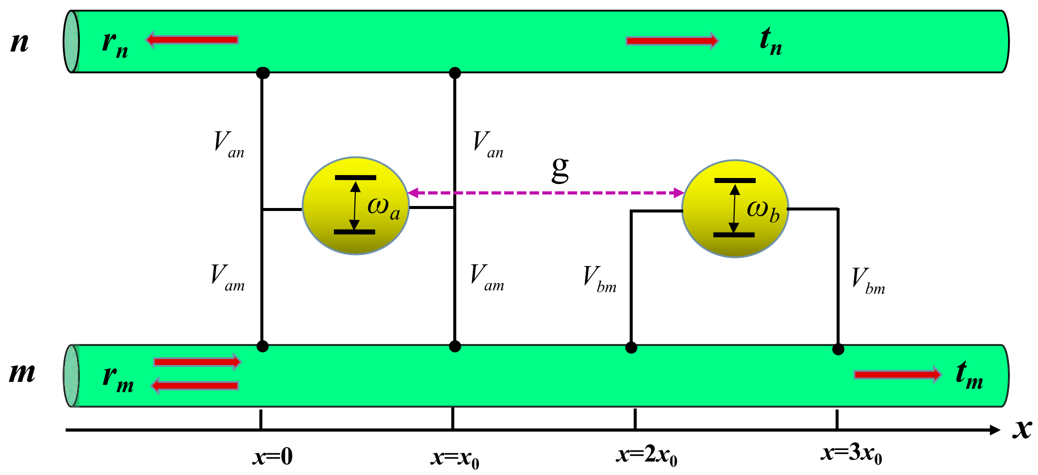

FIGURE 1
Schematic configuration of routing single photons in two channels made of two infinite linear waveguides. The giant two-level atom *a* couples twice with the waveguide *m* (waveguide *n*) at $x = 0$ and $x = x_0$ with strength V_{am} (V_{an}), and the giant two-level atom *b* only interacts the waveguide *m* at $x = 2x_0$ and $x = 3x_0$ with strength V_{bm}. The purple dashed line indicates an interatomic interaction with strength g. Initially, a single photon is launched from the left side of waveguide *m* and then is reflected, transmitted, or transferred to waveguide *n*.

[39–43], decoherence-free interaction [44–46], chiral quantum optics [47,48], and phase-controlled frequency conversions [49,50]. For a traditional small atom, the size of the atom is very smaller than the wavelength of the field, and thus it can be well described with the dipole approximation. However, a giant atom couples to a waveguide at multiple points, and the distance between these points is no longer negligible compared with the waveguides of propagating fields in the waveguide. Such a giant-atom structure can be realized in several systems, such as superconducting quits coupled to either surface acoustic waves [51–54] or microwave transmission lines [4,44,55–57], cold atoms interacting with optical lattices [58]. In the giant-atom setup, the multiple coupling points lead to additional interference effects that are not present in quantum optics with conventional small atoms [37,39,45,59,60].

It is very interesting to study the issue that how to mediate single-photon scattering by the giant atoms. Some pioneering works have been reported in this area [42,50,61–65]. Reference [42] investigated the single-photon scattering properties in a one-dimensional coupled-resonator waveguide, where a giant two-level atom is nonlocally coupled to the waveguide *via* two or multiple resonators. The results showed that a giant atom can be treated as a controller to manipulate the propagation of the photon by introducing the interference effect. In a giant-molecule waveguide-QED system consisting of two coupled giant atoms and an infinite waveguide, the single-photon scattering in both the Markovian and non-Markovian regimes was studied. In this system, the asymmetric Fano line-shapes and the Rabi splitting-like phenomenon were observed [61]. Zhao et.al., reported that single photon scattering in a one-dimensional waveguide can be dynamically controlled by the periodic phase modulation *via* changing the size of the giant atom and a tunable Autler-Townes splitting can be achieved with the giant atom [62]. Furthermore, a chiral giant-atom model in both the Markovian and the non-Markovian regimes was focused, and it was shown that intriguing interference effects induced by a giant-atom structure result in exotic quantum phenomena such as ultranarrow scattering window [50].

Very recently, the strong dependence of single photon routing properties on the size of a giant atom coupling to two waveguides was revealed. To improve the routing efficiency, a perfect mirror was placed into the non-target waveguide to form a boundary and then the routing efficiency can reach unity [63]. An alternative approach was proposed in Ref. [21] to achieve a high transfer-rate routing, which is to place an atomic mirror aside the input channel but not to terminate it. Inspired by these works, we show an extension of the single photon router based on a single giant atom to the router with two coupled giant atoms, one of which serves as an atomic mirror. With the real-space approach, the exact expressions of the single-photon transmission and reflection amplitudes are derived. We explore the dependence of the single photon properties on the phase shift between two atom-waveguide coupling points, the frequency detuning between the incident photon and the atoms, the coupling strength between the two giant atoms, and the interaction strengths between the atoms and the waveguides. It is found that the single photon incident from one waveguide can be redirected in the other waveguide with a 100% probability by well designing the size of the giant atom and the frequency detuning or adjusting the ratio between the two atom-waveguide coupling strengths.

The paper is organized as follows: In Section 2, we present theoretical model and give the exact expressions of the single-photon transmission and reflection amplitudes with the real-space approach. In Section 3, we discuss the effects of the phase shift between two adjacent coupling points, the frequency detuning, the atomic interaction, and the coupling strengths between the giant atoms and the waveguides on the single photon routing properties. Finally, we conclude with a brief summary of the results in Section 4.

2 Theoretical model

As shown in Figure 1, we consider a single-photon router composed of two infinite linear waveguides and two coupled giant two-level atoms. The giant atom a simultaneously couples to the two waveguides, waveguide m and waveguide n, at two points $x = 0$ and $x = x_0$, respectively, while the giant atom b only interacts the waveguide m at $x = 2x_0$ and $x = 3x_0$. For simplicity, we assume here that the distances between any two neighboring connection points are identical. With rotating-wave approximation [66,67], the real-space Hamiltonian of the system could be written as ($\hbar = 1$)

$$H = H_w + H_{ab} + H_I, \tag{1}$$

where H_w represents the free Hamiltonian of the two waveguides, H_{ab} describes the two coupled giant atoms, H_I is the interaction Hamiltonian between the atoms and the waveguides. The expressions of these Hamiltonian are written as follows:

$$H_w = \sum_{s=m,n} \int dx \left[c^+_{R_s}(x)\left(-iv_g\frac{\partial}{\partial x}\right)c_{R_s}(x) + c^+_{L_s}(x)\left(iv_g\frac{\partial}{\partial x}\right)c_{L_s}(x)\right], \tag{2}$$

$$H_{ab} = \omega_a\sigma_a^+\sigma_a^- + \omega_b\sigma_b^+\sigma_b^- + g\left(\sigma_a^+\sigma_b^- + \sigma_b^+\sigma_a^-\right), \tag{3}$$

$$H_I = \sum_{s=m,n} V_{as}\int dx[\delta(x) + \delta(x-x_0)]\left[c^+_{R_s}(x)\sigma_a^- + c^+_{L_s}(x)\sigma_a^- + H.c.\right] + V_{bm}\int dx[\delta(x-2x_0) + \delta(x-3x_0)] \times \left[c^+_{R_m}(x)\sigma_b^- + c^+_{L_m}(x)\sigma_b^- + H.c.\right], \tag{4}$$

where $c^+_{R_s}(x)$ $(c_{R_s}(x))$and $c^+_{L_s}(x)$ $(c_{L_s}(x))$ $(s = m, n)$ are the bosonic creation (annihilation) operators of the right- and left-propagating photons at position x in the waveguide s, respectively. v_g is the group velocity of the photons. ω_a (ω_b) is the atomic transition frequency for the atom a (b). σ_a^+ (σ_b^+) and σ_a^- (σ_b^-) are the raising and lowering operators for the atom a (b). g characterizes the intensity of the interaction between the two giant atoms. V_{as} (V_{bs}) is the coupling strength between the atom a (b) and the waveguide s ($s = m, n$). The Dirac delta functions $\delta(x)$ and $\delta(x - x_0)$ indicate that the giant atom a interacts with the two waveguides *via* two points $x = 0$ and $x = x_0$, respectively. The functions $\delta(x - 2x_0)$ and $\delta(x - 3x_0)$ represent that the giant atom b couples to the waveguide m at $x = 2x_0$ and $x = 3x_0$. $H.\,c.$ stands for the Hermitian conjugate.

We assume that initially a single photon with energy $v_g k$ is injected from the far left of the waveguide m. In the single-excitation subspace, the eigenstate of the system can be written as

$$|\omega\rangle = \sum_{s=m,n}\int dx\left[\phi_{R_s}(x)c^+_{R_s}(x) + \phi_{L_s}(x)c^+_{L_s}(x)\right]|\varnothing\rangle + u_a\sigma_a^+|\varnothing\rangle + u_b\sigma_b^+|\varnothing\rangle, \tag{5}$$

where $|\varnothing\rangle$ is the vacuum state, which indicates zero photon in any waveguide and the two giant atoms in their ground states. u_a (u_b) is excitation amplitude of the atom a (b) in the excite state $|e\rangle_a$ ($|e\rangle_b$). $\phi_{R_s}(x)$ and $\phi_{L_s}(x)$ $(s = m, n)$ are, respectively, the probability amplitudes of the right- and left-propagating photons in the waveguide s. They have the following forms:

$$\phi_{R_m}(x) = e^{ikx}[\theta(-x) + t_{m1}\theta(x)\theta(x_0-x) + t_{m2}\theta(x-x_0)\theta(2x_0-x) + t_{m3}\theta(x-2x_0)\theta(3x_0-x) + t_m\theta(x-3x_0)], \tag{6}$$

$$\phi_{L_m}(x) = e^{-ikx}[r_m\theta(-x) + r_{m1}\theta(x)\theta(x_0-x) + r_{m2}\theta(x-x_0)\theta(2x_0-x) + r_{m3}\theta(x-2x_0)\theta(3x_0-x)], \tag{7}$$

$$\phi_{R_n}(x) = e^{ikx}[t_{n1}\theta(x)\theta(x_0-x) + t_n\theta(x-x_0)], \tag{8}$$

$$\phi_{L_n}(x) = e^{-ikx}[r_n\theta(-x) + r_{n1}\theta(x)\theta(x_0-x)], \tag{9}$$

where $\theta(x)$ is the Heaviside step function. t_m (t_n) and r_m (r_n) are, respectively, the transmission and reflection coefficients in the waveguide m (n). t_{mj} (t_{nj}) and r_{mj} (r_{nj}) represent the probability amplitudes for right-going and left-going photons between $x = (j-1)x_0$ and $x = jx_0$ ($j = 1, 2, 3$) in the waveguide m (n), respectively.

Solving the eigenvalue equation $H|\omega\rangle = \omega|\omega\rangle$ with the expressions in Eqs 2–9, one can obtain a set of equations

$$\begin{aligned}
&V_{am}u_a - iv_g(t_{m1} - 1) = 0,\\
&V_{am}u_a - iv_g e^{i\theta}(t_{m2} - t_{m1}) = 0,\\
&V_{am}u_a + iv_g(r_{m1} - r_m) = 0,\\
&V_{am}u_a + iv_g e^{-i\theta}(r_{m2} - r_{m1}) = 0,\\
&V_{an}u_a - iv_g t_{n1} = 0,\\
&V_{an}u_a - iv_g e^{i\theta}(t_n - t_{n1}) = 0,\\
&V_{an}u_a + iv_g(r_{n1} - r_n) = 0,\\
&V_{an}u_a - iv_g e^{-i\theta}r_{n1} = 0,\\
&V_{bm}u_b - iv_g e^{2i\theta}(t_{m3} - t_{m2}) = 0,\\
&V_{bm}u_b - iv_g e^{3i\theta}(t_m - t_{m3}) = 0,\\
&V_{bm}u_b + iv_g e^{-2i\theta}(r_{m3} - r_{m2}) = 0,\\
&V_{bm}u_b - iv_g e^{-3i\theta}r_{m3} = 0,
\end{aligned}$$

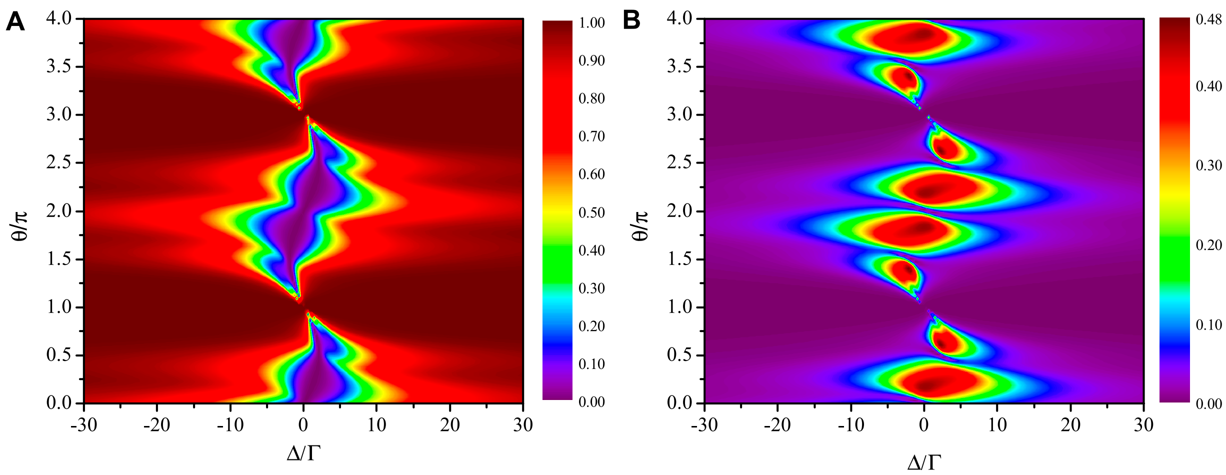

FIGURE 2
Transmission rates T_m **(A)** and T_n **(B)** as a function of the detuning Δ and the phase shift θ, in which the frequency detunings are equal ($\Delta_a = \Delta_b = \Delta$), and the two atom-waveguide coupling strengths are the same ($\Gamma_a = \Gamma_b = \Gamma$). A dark purple sinusoidal shape implies $T_m = 0$, and T_n can reach its maximum value of 0.48. The transferred rate $T_n + R_n$ ($R_n = T_n$) of the photon from the input waveguide m into the targeted waveguide n is 0.96. The other parameter is g = 0.

$$\begin{aligned} &gu_a - \Delta_b u_b + V_{bm}\left(t_{m2}e^{2i\theta} + r_{m2}e^{-2i\theta} + t_m e^{3i\theta}\right) = 0, \\ &gu_b - \Delta_a u_a + V_{am}\left(1 + r_m + t_{m1}e^{i\theta} + r_{m1}e^{-i\theta}\right) \\ &\quad + V_{an}\left(r_n + t_{n1}e^{i\theta} + r_{n1}e^{-ik\theta}\right) \\ &\quad = 0, \end{aligned} \tag{10}$$

where $\Delta_a = \omega - \omega_a$ and $\Delta_b = \omega - \omega_b$ are the frequency detunings between the incident photon and the atom a and b, respectively. $\theta = kx_0$, describes an accumulated phase of single photon traveling between any two adjacent coupling points. Then one can get the transmission and reflection amplitudes

$$t_m = \frac{(\Delta_b - 2\Gamma_b \sin\theta)Q_1 - 2g\sqrt{\Gamma_a\Gamma_b}Q_2 - g^2}{i(1 + e^{i\theta})Q_3 + \Delta_a\Delta_b - g^2} \tag{11}$$

$$r_m = \frac{-(1 + e^{i\theta})^2\left(\Gamma_a\Delta_b + \Gamma_b\Delta_a e^{4i\theta} + 2g\sqrt{\Gamma_a\Gamma_b}\,e^{2i\theta} + 2i\Gamma_a\Gamma_b Q_4\right)}{(1 + e^{i\theta})Q_3 - i\left(\Delta_a\Delta_b - g^2\right)}, \tag{12}$$

$$t_n = r_n e^{-i\theta} = \frac{e^{-i\theta}(1 + e^{i\theta})^2\left(\Gamma_a\Delta_b + g\sqrt{\Gamma_a\Gamma_b}\,e^{2i\theta} - i\Gamma_a\Gamma_b Q_5\right)}{(1 + e^{i\theta})Q_3 - i\left(\Delta_a\Delta_b - g^2\right)}, \tag{13}$$

where $\Gamma_a = V_{am}^2/v_g = V_{an}^2/v_g$ and $\Gamma_b = V_{bm}^2/v_g$, respectively, are the decay rates from the atom a and b into the waveguides. Then Γ_a (Γ_b) characterizes the coupling strength between the atom a (b) and the waveguides. Here, we assume $V_{an} = V_{am}$ for simplicity. We introduce the notations Q_j (j = 1, 2, 3, 4, 5) as follows: $Q_1 = \Delta_a + 2i\Gamma_a(1 + \cos\theta + 2i\sin\theta)$, $Q_2 = \sin\theta + 2\sin 2\theta + \sin 3\theta$, $Q_3 = 2g\sqrt{\Gamma_a\Gamma_b}e^{i\theta}(1 + e^{i\theta}) + 2(\Gamma_b\Delta_a + 2\Gamma_a\Delta_b) + i\Gamma_a\Gamma_b(1 + e^{i\theta})\left[8 - e^{2i\theta}(1 + e^{i\theta})^2\right]$, $Q_4 = 1 + e^{3i\theta}(2\cos 2\theta - 1)$, $Q_5 = e^{3i\theta}(1 + e^{i\theta})^2 - 2(1 + e^{i\theta})$.

Based on Eqs 11–13, the single-photon transmission and reflection rates could be defined by

$$T_s = |t_s|^2, \quad R_s = |r_s|^2, \quad (s = m, n). \tag{14}$$

One can obtian the relations $R_n = T_n$ and $R_m + T_m + R_n + T_n = 1$ for probability conservation.

3 Single photon scattering mediated by two giant atoms

Now, we explore the single photon routing properties between the two waveguides mediated by the two giant atoms. Here, we interest in the quantum transfer efficiency $R_n + T_n$ from the waveguide m to n, and only focus on T_n due to the relation $R_n = T_n$. The simple case with $\Delta_a = \Delta_b = \Delta$, $\Gamma_a = \Gamma_b = \Gamma$ and g = 0 is considered firstly. In this case, the transmission and reflection amplitudes in Eqs 11–13 can be simplified as

$$t_m = \frac{(\Delta - 2\Gamma\sin\theta)Q_1'}{i(1 + e^{i\theta})Q_3' + \Delta^2} \tag{15}$$

$$r_m = \frac{-\Gamma(1 + e^{i\theta})^2\left[\Delta(1 + e^{4i\theta}) + 2i\Gamma Q_4\right]}{(1 + e^{i\theta})Q_3' - i\Delta^2}, \tag{16}$$

$$t_n = r_n e^{-i\theta} = \frac{\Gamma e^{-i\theta}(1 + e^{i\theta})^2(\Delta - i\Gamma Q_5)}{(1 + e^{i\theta})Q_3' - i\Delta^2}, \tag{17}$$

where $Q_1' = \Delta + 2i\Gamma(1 + \cos\theta + 2i\sin\theta)$, $Q_3' = 6\Gamma\Delta + i\Gamma^2(1 + e^{i\theta})\left[8 - e^{2i\theta}(1 + e^{i\theta})^2\right]$.

Figure 2 displays the transmission rates T_m and T_n *versus* the detuning Δ between the incident photon and the atoms, and the phase shift θ between two adjacent atom-waveguide coupling points. Here, the coupling strength between the two atoms is not taken into account, *i.e.*, g = 0. Obviously, these spectra vary

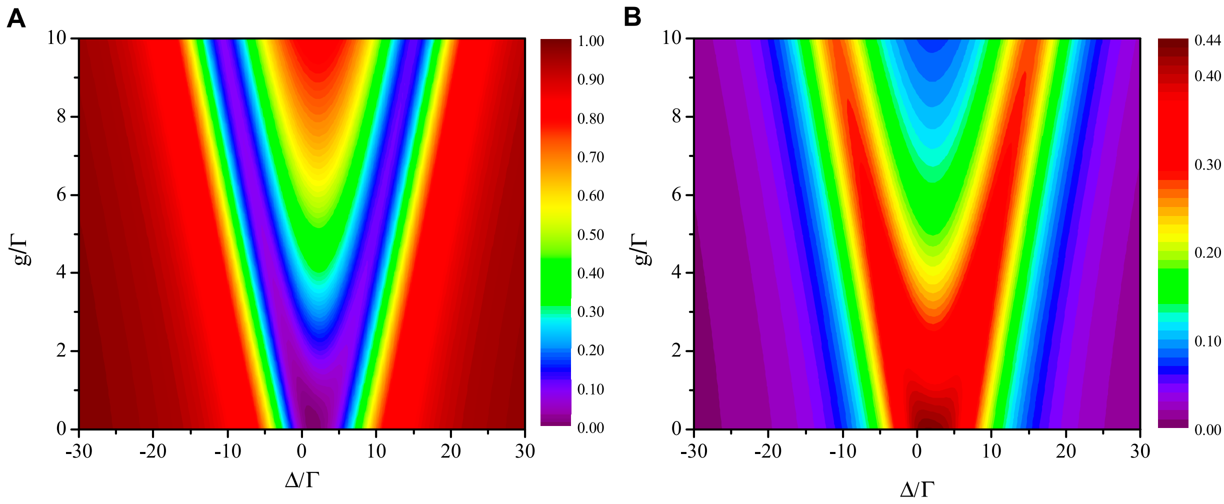

FIGURE 3
Transmission rates T_m **(A)** and T_n **(B)** as a function of the detuning Δ and the coupling strength g between the two atoms under the same atom-waveguide interaction strengths ($\Gamma_a = \Gamma_b = \Gamma$). The spectra show V-type shapes, indicating the existence of two valleys or peaks. The phase shift between two adjacent coupling points is fixed to $\theta = \pi/4$.

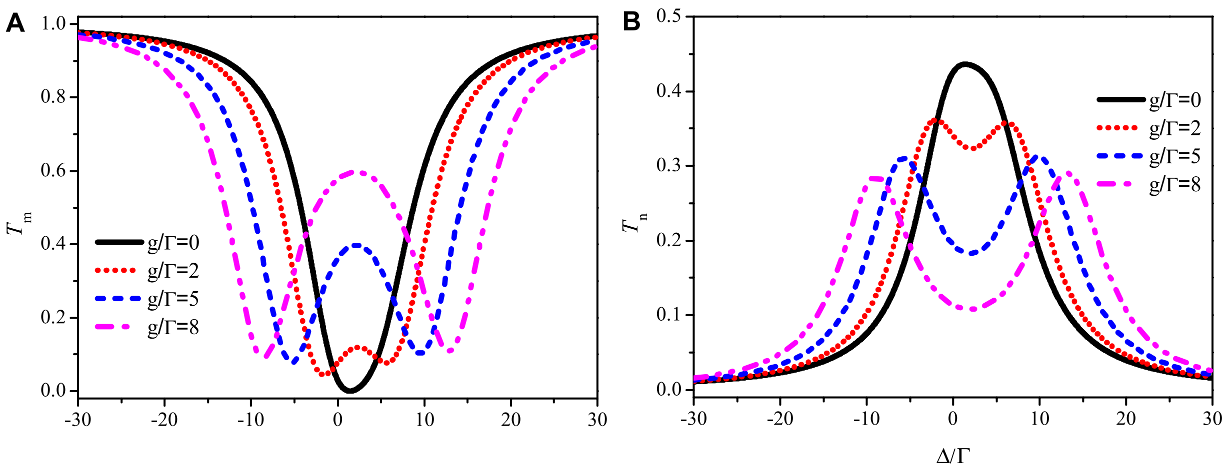

FIGURE 4
The transmitted curves T_m **(A)** and T_n **(B)** show the profiles of Figure 3. The effect of the coupling strength g between the atom *a* and *b* on the single-photon scattering is revealed. The number of valleys or peaks varies from one to two as g changes from zero to non-zero.

periodically as θ with a period of 2π. Note that the value of T_m is always zero when $\Delta = 2\Gamma \sin\theta$, except for some special phases $\theta = (2j - 1)\pi$ ($j = 1, 2, 3 \ldots$) by analyzing Eq. 15. A dark purple sinusoidal shape appears at $\Delta/\Gamma = 2 \sin\theta$, indicating $T_m = 0$, as shown in Figure 2A. Similar transmitted behavior have also been demonstrated in other giant-atom setups [50,62,68]. In the case of $\theta = (2j - 1)\pi$ ($j = 1, 2, 3 \ldots$), we have $R_m = T_n = R_n = 0$ (R_m and R_n not shown in Figure 2) with the factor $1 + e^{i\theta} = 0$ in the expressions of Eqs 16, 17 but $T_m = 1$. The perfect transmission of the single photon arises from the quantum interferences among the multiple connection points [45]. Figure 2B displays that T_n can reach a maximum value of 0.48 ($R_n = T_n = 0.48$), which can be verified by numerical calculation based on Eq. 17. The results indicate that the maximum total quantum routing probability ($R_n + T_n$) from waveguide m to waveguide n is about 0.96.

As shown in Figures 3, 4, we plot the effect of the coupling strength between the two giant atoms on single-photon routing properties. We also assume $\Delta_a = \Delta_b = \Delta$ and $\Gamma_a = \Gamma_b = \Gamma$. Figure 3

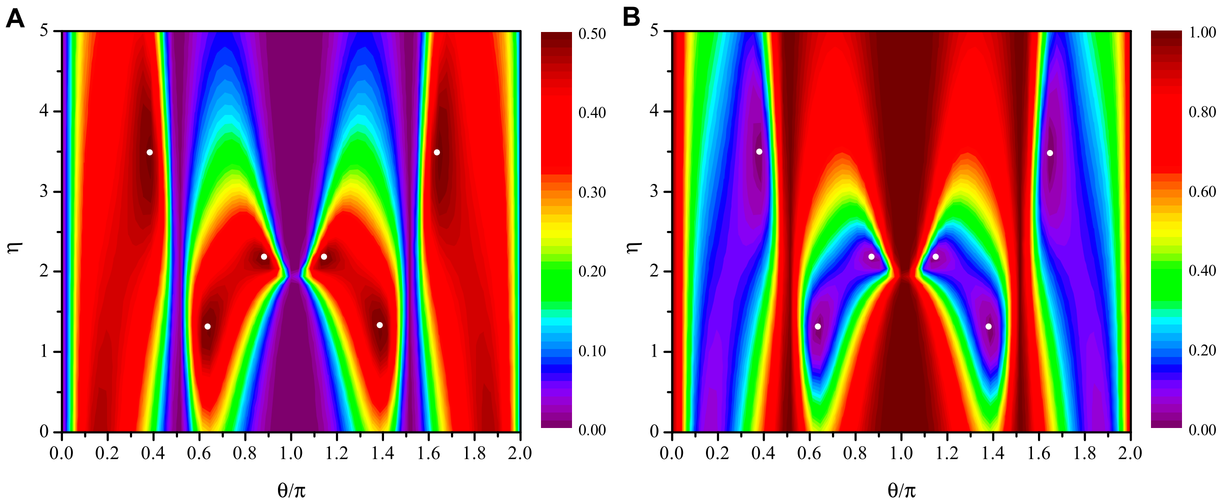

FIGURE 5
The extreme values of T_n **(A)** and R_m **(B)** for various phase shift θ and the ratio η between the two atom-waveguide coupling strengths. White dots represent extremum points with $T_n = 0.5$ or $R_m = 0$, showing symmetric about $\theta = \pi$. The values of the parameters at the six extreme points are listed in Table 1. The interatomic interaction is fixed to g = 0.

TABLE 1 The values of the parameters θ, η and Δ at extremum points with $T_n = R_n = 0.5$ and $T_m = R_m = 0$ in Figures 5, 6.

θ	$3\pi/8$	$5\pi/8$	$7\pi/8$	$9\pi/8$	$11\pi/8$	$13\pi/8$
η	3.50	1.33	2.20	2.20	1.33	3.50
Δ/Γ	6.46	2.46	1.68	−1.68	−2.46	−6.46

exhibits the transmission rates T_m and T_n as a function of the detuning Δ and the coupling strength g. One can see that there are two valleys or peaks, which are more clearly demonstrated by the profiles of Figure 3, as depicted in Figure 4. When g = 0, there is a single valley or peak in these scattering spectra, but for g ≠ 0 two valleys or peaks appear in these spectra. As g increases, the separation of the two valleys or peaks gradually increases and the intensities also change. The results indicate that the coupling strength between the two atoms can control the single-photon scattering in the two waveguide channels. However, an increase of the coupling strength leads to decreasing of T_n. Consequently, when the coupling strength g = 0 the maximum total quantum routing probability with 0.88 can reach.

Next, the influence of the atom-waveguide coupling strengths on single-photon routing properties is investigated. Here, we also set $\Gamma_a = \Gamma$, serving as the unit of other parameters, but change the value of Γ_b by adjusting the ratio $\Gamma_b/\Gamma_a = \eta$. Moreover, the interatomic coupling is turned off, *i.e.,* g = 0. To explore a possible unit transfer efficiency from the waveguide m to n, we let $\Delta = 2\Gamma_b \sin\theta = 2\Gamma\eta\sin\theta$ $[\theta \neq (2j-1)\pi, j = 1, 2, 3 \ldots]$ to ensure $T_m = 0$, meanwhile, seek the condition of $R_m = 0$. After analyzing Eqs 11, 12, both $T_m = 0$ and $R_m = 0$ are guaranteed when the following conditions are satisfied simultaneously:

$$\Delta = 2\Gamma\eta\sin\theta, \tag{18}$$

$$\Delta = \frac{-2\Gamma[1+\cos 3\theta(2\cos 2\theta - 1)]}{\sin 4\theta}, \tag{19}$$

$$\eta = \frac{1+\cos 3\theta(2\cos 2\theta - 1)}{\Gamma[\cos\theta(1-2\cos 2\theta) - \cos 4\theta]}, \tag{20}$$

To clearly demonstrate possible extremum values of T_n and R_m, we plot T_n and R_m as a function of θ and η by substituting g = 0 and $\Delta = 2\Gamma_b\sin\theta$ into Eqs 11–13. One can see that there are six extremum points with $T_n = 0.5$ and $R_m = 0$ marked with white dots in Figures 5A,B, respectively, and they are symmetric about $\theta = \pi$. The exact locations of the six extreme points are obtained based on the numerical analysis of Eqs 18–20, as shown in Table 1. We plot T_m, R_m and T_n *versus* Δ where the values of the other parameters are provided in the Table. It is worth noting that each pair of spectra (*i.e.,* Figures 6A–F) with the same values of η are symmetric with respect to the vertical line $\Delta = 0$. In fact, we have $T_m\,[\eta, -\Delta, 2\pi-(2j-1)\pi/8] = T_m\,[\eta, \Delta\,(2j-1)\pi/8]$, $R_m\,[\eta, -\Delta, 2\pi-(2j-1)\pi/8] = R_m\,[\eta, \Delta\,(2j-1)\pi/8]$ and $T_n\,[\eta, -\Delta,$

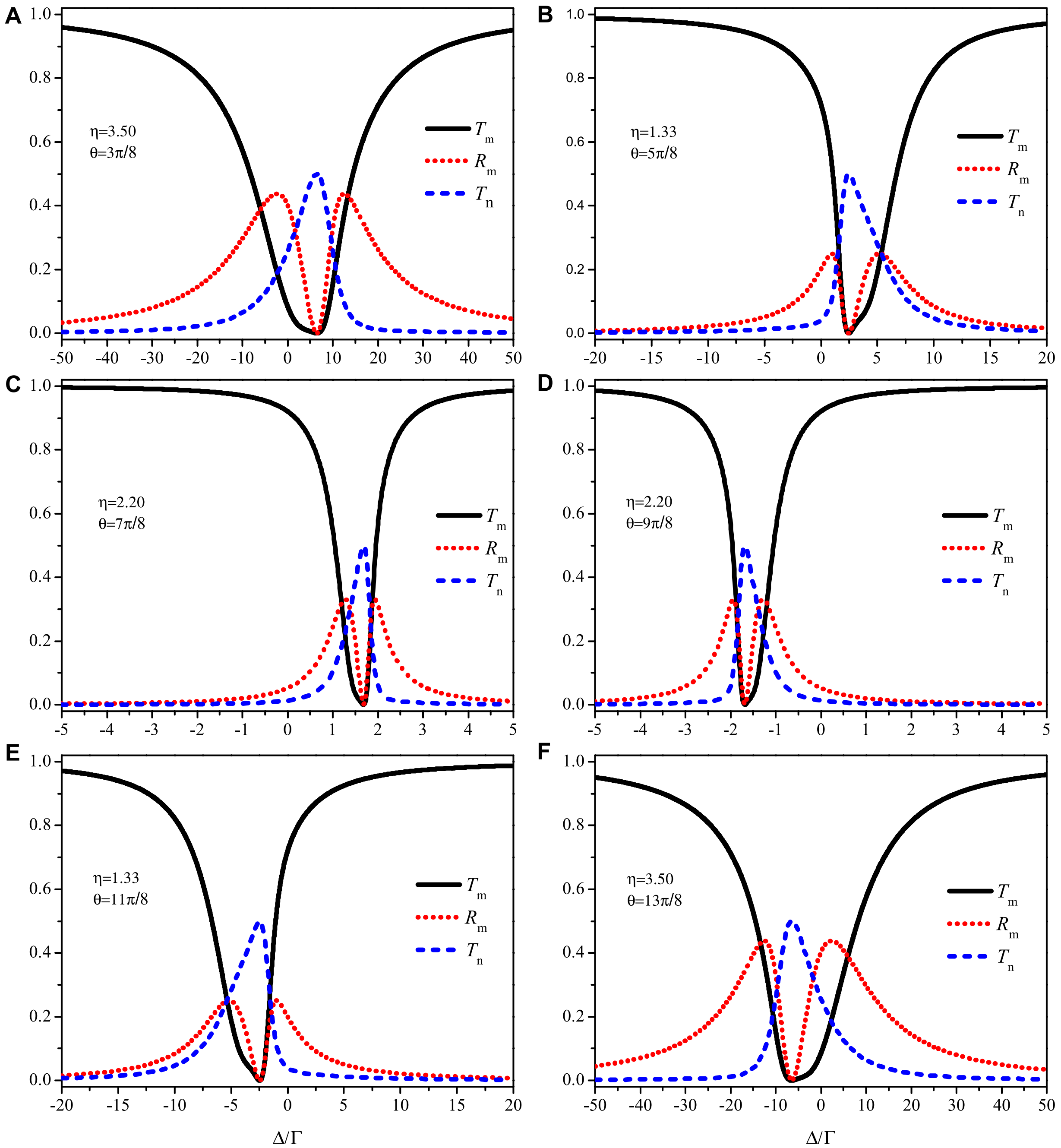

FIGURE 6
Transmission and reflection rates T_m (dark solid line), T_n (blue dashed line) and R_m (red dotted line) as a function of Δ around the six extreme points shown in Figure 5. **(A)** $\eta = 3.50$, $\theta = 3\pi/8$, **(B)** $\eta = 1.33$, $\theta = 5\pi/8$, **(C)** $\eta = 2.20$, $\theta = 7\pi/8$, **(D)** $\eta = 2.20$, $\theta = 9\pi/8$, **(E)** $\eta = 1.33$, $\theta = 11\pi/8$, **(F)** $\eta = 3.50$, $\theta = 13\pi/8$. The transmitted spectra of T_m and T_n show a single valley or peak, while the reflected spectrum of R_m exhibits two peaks. The values of η and θ are provided by Table 1 and the interatomic interaction is not considered (g = 0).

$2\pi - (2j-1)\pi/8] = T_n\,[\eta, \Delta\,(2j-1)\pi/8]$ $(j = 2, 3, 4, 5, 6, 7)$. In addition, two peaks appear in the reflected spectra R_m but not in other spectra. The locations of the two peaks are derived as $\Delta_\pm = (\eta+2)\sin\theta \pm \sqrt{(\eta+2)^2\sin^2\theta + \eta Q}$ with $Q = 8 + 16\cos\theta + 7\cos 2\theta - 4\cos 3\theta - 6\cos 4\theta - 4\cos 5\theta - \cos 6\theta$, where the values of the parameters θ and η are given by Table 1. These results mean that the single photon transfer efficiency from the waveguide m to n can reach 100% (*i.e.,* $R_n + T_n = 1$) by designing a proper size of the giant atom, and adjusting the atom-waveguide coupling strength and the frequency detuning between the atoms and the single photon. Different from the single-photon router containing a small-atom mirror in Ref. [21],

TABLE 2 The values of the parameters θ, Δ_a and Δ_b with $T_n = R_n = 0.5$ and $T_m = R_m = 0$ in Figure 7.

θ	$\pi/8$	$3\pi/8$	$5\pi/8$	$7\pi/8$	$9\pi/8$	$11\pi/8$	$13\pi/8$	$15\pi/8$
Δ_a/Γ	−2.32	6.46	2.46	1.68	−1.68	−2.46	−6.46	2.32
Δ_b/Γ	0.76	1.85	1.85	0.76	−0.76	−1.85	−1.85	−0.76

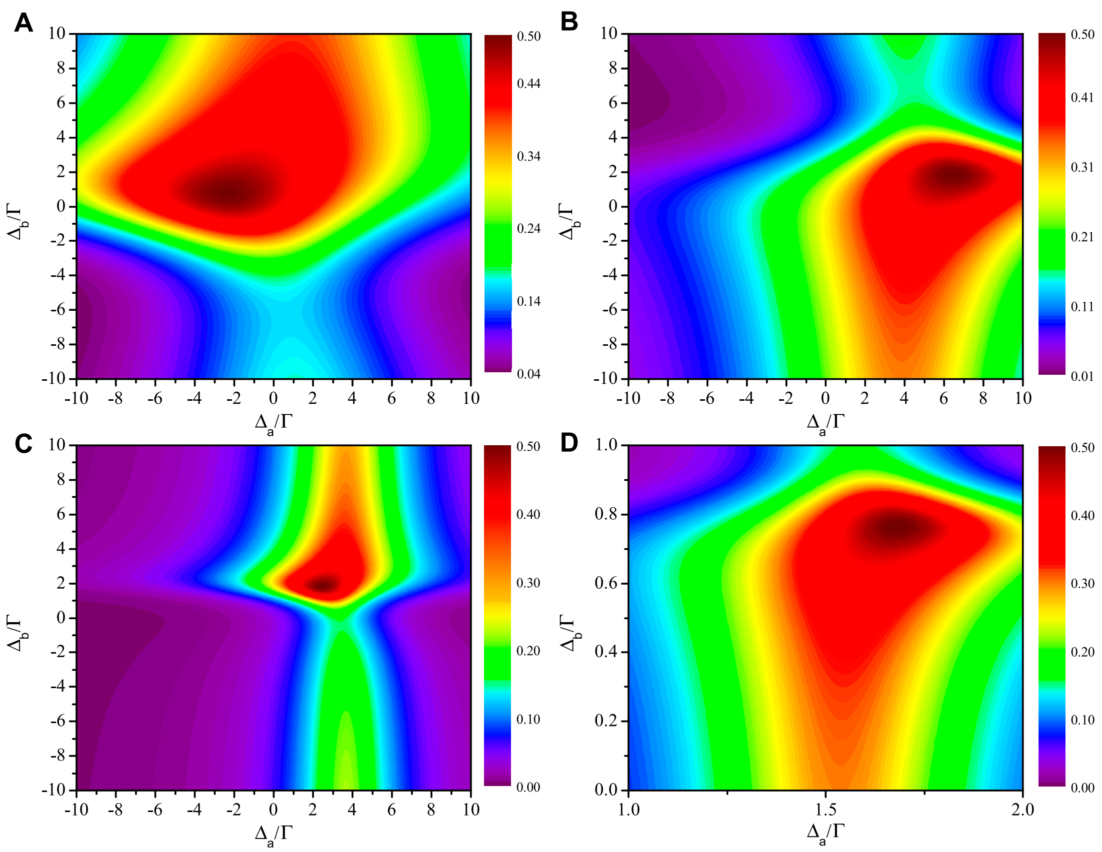

FIGURE 7
Transmission rate T_n as a function of Δ_a and Δ_b, in which the four values of the phase shift θ are given by Table 2. Specially, **(A)** $\theta = \pi/8$, **(B)** $\theta = 3\pi/8$, **(C)** $\theta = 5\pi/8$, **(D)** $\theta = 7\pi/8$. The transmitted spectra with the other four values of θ are not presented here. The total transfer efficiency from the waveguide m to n can achieve 100% by adjusting the detunings. The other parameters are $\Gamma_a = \Gamma_b = \Gamma$, $g = 0$.

we introduce two coupled giant atoms to mediate the single-photon routing between two infinite waveguides, where a giant atom is located between the two waveguides to transfer the single photon from the input waveguide m to the output waveguide n, and the other one only interacts with the non-target waveguide m to serve as a giant-atom mirror.

Finally, we explore the effects of the detunings Δ_a and Δ_b on the single photon quantum routing. After analyzing Eqs 11–13 and letting $g = 0$, $\Gamma_a = \Gamma_b = \Gamma$, a single photon router with unit efficiency may be achieved when the following equations are fulfilled

$$\Delta_b - 2\Gamma \sin\theta = 0, \tag{21}$$

$$\Delta_a \sin 4\theta + 2\Gamma[1 - \cos 3\theta(1 - 2\cos 2\theta)] = 0, \tag{22}$$

$$\Delta_b + 2\Gamma(1 - 2\cos 2\theta)(\sin 3\theta + \cos 3\theta \cot 4\theta) - 2\Gamma \cot 4\theta = 0, \tag{23}$$

The calculation and analysis for the above equations show that there are eight solutions of θ meeting the conditions, specially, $\theta = (2j - 1)\pi/8$, $(j = 1, 2, 3, 4, 5, 6, 7, 8)$, and the other parameters are listed in Table 2. One can find that there is the relation $T_n[-\Delta_a, -\Delta_b, 2\pi - (2j-1)\pi/8] = T_n[\Delta_a, \Delta_b, (2j-1)\pi/8]$. As a consequence, any two transmitted spectra with $\theta = (2j-1)\pi/8$ and $2\pi - (2j-1)\pi/8$ show central symmetry with respect to the origin ($\Delta_a = 0, \Delta_b = 0$). Figure 7 shows the transmission rate T_n *versus* Δ_a and Δ_b with some given values of θ provided by Table 2. This indicates that a single photon router with unit efficiency can be also realised by tuning the phase shift of two adjacent connection points and the frequency detuning between the single photon and the atoms.

4 Conclusion

We have studied the influence of two coupled giant two-level atoms on the modulation of single photon quantum routing in two channels composed of two infinite waveguides, and derived the exact expressions of the single-photon transmission and reflection amplitudes with the real-space approach. Our studies show the single photon scattering can be mediated by the atomic phase difference, the frequency detuning, the interatomic interaction, and the coupling strengths between the giant atoms and the waveguides. In the two-giant-atom scheme, it is found that the giant atom located between the two waveguides plays a role in transferring the single photon from the input waveguide to the output waveguide, and the other one interacting with the non-target waveguide is equivalent to a giant-atom mirror, inducing additional interferences. Importantly, a single photon router with unit efficiency can be realised by designing a proper size of the giant atom and adjusting the ratio of the coupling strength and the frequency detuning. Our work may provide a feasible approach to design an efficient quantum router and manipulate photon transport at the single-photon level using the giant-atom setup.

Data availability statement

The original contributions presented in the study are included in the article/Supplementary Material, further inquiries can be directed to the corresponding author.

Author contributions

YZ and ZZ conceived the physical model and the idea of the study, and ZZ and ZP performed the numerical calculation and numerical analysis. ZZ and WY contributed to writing the manuscript. All authors contributed to manuscript revision, read, and approved the submitted version.

Funding

This work was partly supported by Scientific Research Fund of Hunan Provincial Education Department under Grant Nos 19B206, 21B0485, the National Natural Science Foundation of China under Grant Nos 11704115, 11504104, 51867002, 61835013, and the Hunan Provincial Natural Science Foundation of China Grant No. 2021JJ40188.

Acknowledgments

The authors thank C. X. Jia and C. L. Jiang for helpful discussions.

Conflict of interest

The authors declare that the research was conducted in the absence of any commercial or financial relationships that could be construed as a potential conflict of interest.

Publisher's note

References

1. Kimble HJ. The quantum internet. *Nature* (2008) 453:1023–30. doi:10.1038/nature07127

2. O'Brien JL, Furusawa A, Vučković J. Photonic quantum technologies. *Nat Photon* (2009) 3:687–95. doi:10.1038/nphoton.2009.229

3. Astafiev O, Zagoskin AM, Abdumalikov JA, Pashkin YA, Yamamoto T, Inomata K, et al. Resonance fluorescence of a single artificial atom. *Science* (2010) 327:840–3. doi:10.1126/science.1181918

4. Hoi IC, Wilson CM, Johansson G, Palomaki T, Peropadre B, Delsing P. Demonstration of a single-photon router in the microwave regime. *Phys Rev Lett* (2011) 107:073601. doi:10.1103/PhysRevLett.107.073601

5. Zhou L, Dong H, Liu YX, Sun CP, Nori F. Quantum supercavity with atomic mirrors. *Phys Rev A (Coll Park)* (2008) 78:063827. doi:10.1103/PhysRevA.78.063827

6. Zhou L, Yang S, Liu YX, Sun CP, Nori F. Quantum Zeno switch for single-photon coherent transport. *Phys Rev A (Coll Park)* (2009) 80:062109. doi:10.1103/PhysRevA.80.062109

7. Zhou L, Chang Y, Dong H, Kuang LM, Sun CP. Inherent Mach-Zehnder interference with "which-way" detection for single-particle scattering in one dimension. *Phys Rev A (Coll Park)* (2012) 85:013806. doi:10.1103/PhysRevA.85.013806

8. Zhou L, Yang LP, Li Y, Sun CP. Quantum routing of single photons with a cyclic three-level system. *Phys Rev Lett* (2013) 111:103604. doi:10.1103/PhysRevLett.111.103604

9. Lu J, Zhou L, Kuang LM, Nori F. Single-photon router: Coherent control of multichannel scattering for single photons with quantum interferences. *Phys Rev A (Coll Park)* (2014) 89:013805. doi:10.1103/PhysRevA.89.013805

10. Liao JQ, Gong ZR, Zhou L, Liu YX, Sun CP, Nori F. Controlling the transport of single photons by tuning the frequency of either one or two cavities in an array of coupled cavities. *Phys Rev A (Coll Park)* (2010) 81:042304. doi:10.1103/PhysRevA.81.042304

11. Huang JS, Wang JW, Wang Y, Li YL, Huang YM. Control of single-photon routing in a T-shaped waveguide by another atom. *Quan Inf Process* (2018) 17:78–15. doi:10.1007/s11128-018-1850-9

12. Huang JS, Wang JW, Li YL, Wang Y, Huang YM. Tunable quantum routing via asymmetric in tercavity couplings. *Quan Inf Process* (2019) 18:59–15. doi:10.1007/s11128-019-2176-y

13. Liu L, Zhang JH, Jin L, Zhou L. Transport properties of the non-Hermitian T-shaped quantum router. *Opt Express* (2019) 27:13694–705. doi:10.1364/OE.27.013694

14. Ahumada M, Orellana PA, Domínguez-Adame F, Malyshev AV. Tunable single-photon quantum router. *Phys Rev A (Coll Park)* (2019) 99:033827. doi:10.1103/PhysRevA.99.033827

15. Du XP, Cao Q, Dang N, Tan L. Quantum router modulated by two Rydberg atoms in a X-shaped coupled cavity array. *Eur Phys J D* (2021) 75:79–8. doi:10.1140/epjd/s10053-021-00085-9

16. Tang JS, Nie W, Tang L, Chen MY, Su X, Lu YQ, et al. Nonreciprocal single-photon band structure. *Phys Rev Lett* (2022) 128:203602. doi:10.1103/PhysRevLett.128.203602

17. Cao C, Duan YW, Chen X, Zhang R, Wang TJ, Wang C. Implementation of single-photon quantum routing and decoupling using a nitrogen-vacancy center and a whispering-gallery-mode resonator-waveguide system. *Opt Express* (2017) 25:16931–46. doi:10.1364/OE.25.016931

18. Aoki T, Parkins AS, Alton DJ, Regal CA, Dayan B, Ostby E, et al. Efficient routing of single photons by one atom and a microtoroidal cavity. *Phys Rev Lett* (2009) 102:083601. doi:10.1103/PhysRevLett.102.083601

19. Yang H, Qin GQ, Zhang H, Mao X, Wang M, Long GL. Multimode interference induced optical routing in an optical microcavity. *Annalen der Physik* (2021) 533:2000506. doi:10.1002/andp.202000506

20. Tang L, Tang JS, Chen MY, Nori F, Xiao M, Xia KY. Quantum squeezing induced optical nonreciprocity. *Phys Rev Lett* (2022) 128:083604. doi:10.1103/PhysRevLett.128.083604

21. Li XM, Wei LF. Designable single-photon quantum routings with atomic mirrors. *Phys Rev A (Coll Park)* (2015) 92:063836. doi:10.1103/PhysRevA.92.063836

22. Carlos GB, Esteban M, Francisco JGV, Alejandro GT. Nonreciprocal few-photon routing schemes based on chiral waveguide-emitter couplings. *Phys Rev A (Coll Park)* (2016) 94:063817. doi:10.1103/PhysRevA.94.063817

23. Huang JS, Zhong JT, Li YL, Xu ZH, Xiao QS. Efficient single-photon routing in a double-waveguide system with a mirror. *Quan Inf Process* (2020) 19:290. doi:10.1007/s11128-020-02789-0

24. Yan GA, Lu H. Realization of tunable highly-efficient quantum routing in chiral waveguides. *Front Phys* (2022) 227:880117. doi:10.3389/fphy.2022.880117

25. Yan CH, Li Y, Yuan HD, Wei LF. Targeted photonic routers with chiral photon-atom interactions. *Phys Rev A (Coll Park)* (2018) 97:023821. doi:10.1103/PhysRevA.97.023821

26. Poudyal B, Mirza IM. Collective photon routing improvement in a dissipative quantum emitter chain strongly coupled to a chiral waveguide QED ladder. *Phys Rev Res* (2020) 2:043048. doi:10.1103/PhysRevResearch.2.043048

27. Li XM, Xin J, Li GL, Lu XM, Wei LF. Quantum routings for single photons with different frequencies. *Opt Express* (2021) 29:8861–71. doi:10.1364/OE.418414

28. Kim NC, Ko MC, Ryom JS, Choe H, Choe IH, Ri SR, et al. Single plasmon router with two quantum dots side coupled to two plasmonic waveguides with a junction. *Quan Inf Process* (2021) 20:5–14. doi:10.1007/s11128-020-02884-2

29. Dong MX, Xia KY, Zhang WH, Yu YC, Ye YH, Li EZ, et al. All-optical reversible single-photon isolation at room temperature. *Sci Adv* (2021) 7:eabe8924. doi:10.1126/sciadv.abe8924

30. Lemr K, Bartkiewicz K, Cernoch A, Soubusta J. Resource-efficient linear-optical quantum router. *Phys Rev A (Coll Park)* (2013) 87:062333. doi:10.1103/PhysRevA.87.062333

31. Xia K, Jelezko F, Twamley J. Quantum routing of single optical photons with a superconducting flux qubit. *Phys Rev A (Coll Park)* (2018) 97:052315. doi:10.1103/PhysRevA.97.052315

32. Wen PY, Kockum AF, Ian H, Chen JC, Nori F, Hoi IC. Reflective amplification without population inversion from a strongly driven superconducting qubit. *Phys Rev Lett* (2018) 120:063603. doi:10.1103/PhysRevLett.120.063603

33. Wen PY, Lin KT, Kockum AF, Suri B, Ian H, Chen JC, et al. Large collective Lamb shift of two distant superconducting artificial atoms. *Phys Rev Lett* (2019) 123:233602. doi:10.1103/PhysRevLett.123.233602

34. Wen PY, Ivakhnenko OV, Nakonechnyi MA, Suri B, Lin JJ, Lin WJ, et al. Landau-Zener-Stückelberg-Majorana interferometry of a superconducting qubit in front of a mirror. *Phys Rev B* (2020) 102:075448. doi:10.1103/PhysRevB.102.075448

35. Wang ZL, Wu YK, Bao ZH, Li Y, Ma C, Wang HY, et al. Experimental realization of a deterministic quantum router with superconducting quantum circuits. *Phys Rev Appl* (2021) 15:014049. doi:10.1103/PhysRevApplied.15.014049

36. Ren Y, Ma S, Xie J, Li XK, Cao MT, Li FL. Nonreciprocal single-photon quantum router. *Phys Rev A (Coll Park)* (2022) 105:013711. doi:10.1103/PhysRevA.105.013711

37. Kockum AF, Delsing P, Johansson G. Designing frequency-dependent relaxation rates and Lamb shifts for a giant artificial atom. *Phys Rev A (Coll Park)* (2014) 90:013837. doi:10.1103/PhysRevA.90.013837

38. Guo L, Grimsmo AL, Kockum AF, Pletyukhov M, Johansson G. Giant acoustic atom: A single quantum system with a deterministic time delay. *Phys Rev A (Coll Park)* (2017) 95:053821. doi:10.1103/PhysRevA.95.053821

39. Wang X, Liu T, Kockum AF, Li HR, Nori F. Tunable chiral bound states with giant atoms. *Phys Rev Lett* (2021) 126:043602. doi:10.1103/PhysRevLett.126.043602

40. Guo L, Kockum AF, Marquardt F, Johansson G. Oscillating bound states for a giant atom. *Phys Rev Res* (2020) 2:043014. doi:10.1103/PhysRevResearch.2.043014

41. Guo S, Wang Y, Purdy T, Taylor J. Beyond spontaneous emission: Giant atom bounded in the continuum. *Phys Rev A (Coll Park)* (2020) 102:033706. doi:10.1103/PhysRevA.102.033706

42. Zhao W, Wang ZH. Single-photon scattering and bound states in an atom-waveguide system with two or multiple coupling points. *Phys Rev A (Coll Park)* (2020) 101:053855. doi:10.1103/PhysRevA.101.053855

43. Vega C, Bello M, Porras D, Gonzlez-Tudela A. Qubit-photon bound states in topological waveguides with long-range hoppings. *Phys Rev A (Coll Park)* (2021) 104:053522. doi:10.1103/PhysRevA.104.053522

44. Kannan B, Ruckriegel MJ, Campbell DL, Kockum AF, Braumuller J, Kim DK, et al. Waveguide quantum electrodynamics with superconducting artificial giant atoms. *Nature* (2020) 583:775–9. doi:10.1038/s41586-020-2529-9

45. Kockum AF, Johansson G, Nori F. Decoherence-free interaction between giant atoms in waveguide quantum electrodynamics. *Phys Rev Lett* (2018) 120:140404. doi:10.1103/PhysRevLett.120.140404

46. Carollo A, Cilluffo D, Ciccarello F. Mechanism of decoherence-free coupling between giant atoms. *Phys Rev Res* (2020) 2:043184. doi:10.1103/PhysRevResearch.2.043184

47. Soro A, Kockum AF. Chiral quantum optics with giant atoms. *Phys Rev A (Coll Park)* (2022) 105:023712. doi:10.1103/PhysRevA.105.023712

48. Wang X, Li HR. Chiral quantum network with giant atoms. *Quan Sci Technol* (2022) 7:035007. doi:10.1088/2058-9565/ac6a04

49. Du L, Li Y. Single-photon frequency conversion via a giant Λ-type atom. *Phys Rev A (Coll Park)* (2021) 104:023712. doi:10.1103/PhysRevA.104.023712

50. Du L, Chen YT, Li Y. Nonreciprocal frequency conversion with chiral Λ-type atoms. *Phys Rev Res* (2021) 3:043226. doi:10.1103/PhysRevResearch.3.043226

51. Gustafsson MV, Aref T, Kockum AF, Ekström MK, Johansson G, Delsing P. Propagating phonons coupled to an artificial atom. *Science* (2014) 346:207–11. doi:10.1126/science.1257219

52. Aref T, Delsing P, Ekstrom MK, Kockum AF, Gustafsson MV, Johansson G, et al. Quantum acoustics with surface acoustic waves. In: RH Hadfield G Johansson, editors. *Superconducting devices in quantum optics*. Cham: Springer (2016). p. 217–44.

53. Manenti R, Kockum AF, Patterson A, Behrle T, Rahamim J, Tancredi G, et al. Circuit quantum acoustodynamics with surface acoustic waves. *Nat Commun* (2017) 8:975–6. doi:10.1038/s41467-017-01063-9

54. Andersson G, Suri B, Guo L, Aref T, Delsing P. Non-exponential decay of a giant artificial atom. *Nat Phys* (2019) 15:1123–7. doi:10.1038/s41567-019-0605-6

55. Vadiraj AM, Ask A, McConkey TG, Nsanzineza I, Chang CS, Kockum AF, et al. Engineering the level structure of a giant artificial atom in waveguide quantum

electrodynamics. *Phys Rev A (Coll Park)* (2021) 103:023710. doi:10.1103/PhysRevA.103.023710

56. Blais A, Grimsmo AL, Girvin SM, Wallraff A. Circuit quantum electrodynamics. *Rev Mod Phys* (2021) 93:025005. doi:10.1103/RevModPhys.93.025005

57. Gu X, Kockum AF, Miranowicz A, Liu YX, Nori F. Microwave photonics with superconducting quantum circuits. *Phys Rep* (2017) 718:1–102. doi:10.1016/j.physrep.2017.10.002

58. González-Tudela A, Muñoz CS, Cirac JI. Engineering and harnessing giant atoms in high-dimensional baths: A proposal for implementation with cold atoms. *Phys Rev Lett* (2019) 122:203603. doi:10.1103/PhysRevLett.122.203603

59. Kockum AF, Nori F. Quantum bits with josephson junctions. In: F Tafuri, editor. *Fundamentals and Frontiers of the josephson effect*. Cham: Springer (2019). p. 703–41.

60. Du L, Zhang Y, Wu JH, Kockum AF, Li Y. Giant atoms in a synthetic frequency dimension. *Phys Rev Lett* (2022) 128:223602. doi:10.1103/PhysRevLett.128.223602

61. Yin XL, Liu YH, Huang JF, Liao JQ. Single-photon scattering in a giant-molecule waveguide-QED system. *Phys Rev A (Coll Park)* (2022) 106:013715. doi:10.1103/PhysRevA.106.013715

62. Zhao W, Zhang Y, Wang ZH. Phase-modulated Autler-Townes splitting in a giant-atom system within waveguide QED. *Front Phys (Beijing)* (2022) 17:42506–11. doi:10.1007/s11467-021-1135-0

63. Wang C, Ma XS, Cheng MT. Giant atom-mediated single photon routing between two waveguides. *Opt Express* (2021) 29:40116–24. doi:10.1364/OE.444096

64. Liu N, Wang X, Wang X, Ma XS, Cheng MT. Tunable single photon nonreciprocal scattering based on giant atom-waveguide chiral couplings. *Opt Express* (2022) 30:23428–38. doi:10.1364/OE.460255

65. Chen YT, Du L, Guo LZ, Wang ZH, Zhang Y, Li Y, et al. Nonreciprocal and chiral single-photon scattering for giant atoms. *Commun Phys* (2022) 5:215. doi:10.1038/s42005-022-00991-3

66. Peng JS, Li GX. Effects of the dipole-dipole interaction on dynamic properties and atomic coherent trapping of a two-atom system. *Phys Rev A (Coll Park)* (1993) 47:4212–8. doi:10.1103/PhysRevA.47.4212

67. Shen JT, Fan SH. Theory of single-photon transport in a single-mode waveguide. I. Coupling to a cavity containing a two-level atom. *Phys Rev A (Coll Park)* (2009) 79:023837. doi:10.1103/PhysRevA.79.023837

68. Feng SL, Jia WZ. Manipulating single-photon transport in a waveguide-QED structure containing two giant atoms. *Phys Rev A (Coll Park)* (2021) 104:063712. doi:10.1103/PhysRevA.104.063712